# Reconstructing North Atlantic marine climate variability using an absolutely-dated sclerochronological network

Reynolds, D.J.; Richardson, Christopher; Scourse, James; Butler, Paul; Hollyman, Philip; Román González, Alejandro; Hall, I.R.

**Palaeogeography Palaeoclimatology Palaeoecology**

*DOI:*
10.1016/j.palaeo.2016.08.006

Published: 01/01/2017

Version created as part of publication process; publisher's layout; not normally made publicly available

Palaeogeography, Palaeoclimatology, Palaeoecology xxx (2016) xxx–xxx

Contents lists available at ScienceDirect

Palaeogeography, Palaeoclimatology, Palaeoecology

journal homepage: www.elsevier.com/locate/palaeo

# Reconstructing North Atlantic marine climate variability using an absolutely-dated sclerochronological network

D.J. Reynolds [a,*], C.A. Richardson [b], J.D. Scourse [b], P.B. Butler [b], P. Hollyman [b], A. Román-González [a,b], I.R. Hall [a]

[a] School of Earth and Ocean Science, Cardiff University, Cardiff CF10 3AT, UK
[b] School of Ocean Sciences, College of Natural Science, Bangor University, Menai Bridge, Anglesey LL59 5AB, UK

ARTICLE INFO

*Article history:*
Received 14 January 2016
Received in revised form 1 August 2016
Accepted 2 August 2016
Available online xxxx

*Keywords:*
Sclerochronology
Spatial network
*Arctica islandica*
*Glycymeris glycymeris*
North Atlantic

ABSTRACT

Reconstructing regional to hemispheric-scale climate variability requires the application of spatially representative and climatically sensitive proxy archives. Large spatial networks of dendrochronologies have facilitated the reconstruction of atmospheric variability and inferred variability in the Atlantic Ocean system. However, the marine environment has hitherto lacked the direct application of the spatial network approach because of the small number of individual absolutely-dated marine archives. In this study we present the first analyses of a network of absolutely-dated annually-resolved growth increment width chronologies from the marine bivalves *Glycymeris glycymeris* and *Arctica islandica*. The network contains eight chronologies spanning >500 km along the western British continental shelf from the southern Irish Sea to North West Scotland. Correlation analysis of the individual chronologies and a suite of climate indices, including the Atlantic Multidecadal Oscillation (AMO), Central England surface air temperature (CET), northeast Atlantic sea surface temperatures (SST's) and the winter North Atlantic Oscillation (wNAO), demonstrates that, despite the large geographical distances been sites and the heterogeneous nature of the marine environment, the increment width variability in these series contains an element of coherence likely driven by a common response to changing environmental forcing. A nested Principal component analysis (PCA) was used to construct five composite series which explain between 31% and 74% of the variance across the individual chronologies. Linear regression analyses indicate that the composite series explain up to 41% of the variance in Northeast Atlantic SSTs over the calibration period (1975–2000). Calibration verification (reduction of error [RE] and coefficient of efficiency [CE]) statistics indicate that the composite series contains significant skill at reconstructing multi-decadal northeast Atlantic SST variability over the past two centuries (1805–2010). These data suggest that composite series derived from sclerochronology networks can facilitate the robust reconstruction of marine climate over past centuries to millennia providing invaluable baseline records of natural oceanographic variability.



## 1. Introduction

Developing a detailed understanding of the role the North Atlantic Ocean plays in the wider climate system is essential for developing precise predictions of future climate variability. Evidence derived from instrumental observations suggest that Atlantic variability, associated with changes in SSTs and fluctuations in the strength of the Atlantic Meridional Overturning Circulation (AMOC), is directly linked with broader scale climate variability, including Brazilian and Sahel precipitation (Folland et al., 1986, 2001), Atlantic hurricanes and storm tracks (Goldenberg et al., 2001; Emanuel, 2005), and North American and European temperatures (Sutton and Hodson, 2005; Knight et al., 2006; Mann et al., 2009). Furthermore, evidence derived from palaeoceanographic records suggests that a reduction in the meridional heat transport through the surface components of the AMOC was in part responsible for the reductions in temperatures associated with the Medieval Climate Anomaly (MCA; 1000–1450) to Little Ice Age (LIA; 1450–1850) transition (Lund et al., 2006; Trouet et al., 2009, 2012; Wanamaker et al., 2012; Moffa-Sánchez et al., 2014). With numerical climate model simulations predicting future fluctuations in oceanic heat transport associated with anthropogenic climate forcing (Schmittner et al., 2005; Cheng et al., 2013), there is a growing need to develop a robust quantitative understanding of the role the oceans play in the wider climate system (Haarsma et al., 2013). However, modern observations of the marine environment are limited in their extent, being increasingly sparse both spatially and temporally, and in

* Corresponding author.
*E-mail addresses:* reynoldsd3@cardiff.ac.uk (D.J. Reynolds), c.a.richardson@bangor.ac.uk (C.A. Richardson), j.scourse@bangor.ac.uk (J.D. Scourse), p.g.butler@bangor.ac.uk (P.B. Butler), p_hollyman@hotmail.co.uk (P. Hollyman), roman-gonzalezA@cardiff.ac.uk (A. Román-González), hall@cardiff.ac.uk (I.R. Hall).

http://dx.doi.org/10.1016/j.palaeo.2016.08.006

any case going back no further than CE 1860 (Hurrell and Trenberth, 1999; Smith and Reynolds, 2004). As a result, there is a need to develop precisely-dated and robustly calibrated marine proxy archives that can facilitate the quantitative reconstruction of past ocean changes.

There has been a growing emphasis in the dendrochronological community on the development of spatial networks of tree ring chronologies for the reconstruction of synoptic scale terrestrial climate variability (e.g. Wilson et al., 2016). These networks utilise multiple robustly constructed absolutely-dated dendrochronologies spanning geographical scales from the regional to the hemispheric. The integration of chronologies covering such a wide geographic range allows purely local variability to be averaged out, resulting in a stronger broad scale (regional to hemispheric) climate signal to be deconvolved (Wilson et al., 2010). Such networks have hitherto facilitated the reconstruction of hemispheric surface air temperatures (e.g. Briffa et al., 2002a,b, 2004; Frank and Esper, 2005; Buntgen et al., 2007, 2010), precipitation (e.g. Andreu et al., 2008; Cooper et al., 2013) and interpretations of basin wide marine variability (e.g. Gray, 2004; Mann et al., 2009; Mann et al., 2014; Rahmstorf et al., 2015). Until now this has not been possible for the marine environment because of the limited number of absolutely-dated marine archives. A few recent studies (Cunningham et al., 2013; McGregor et al., 2015) have made use of networks of marine sedimentary archives, dated by means of radiocarbon derived age models. However, these applications are currently limited to lower frequency (multi-decadal to centennial) domains or using binned data due to the typically low resolution and temporal uncertainty associated with marine sediment cores and marine radiocarbon dating. The recent increase in the development of absolutely-dated climatically sensitive sclerochronological records (e.g. Brocas et al., 2013; Butler et al., 2013; Reynolds et al., 2013), derived from the annually resolved growth increments contained in long-lived marine bivalve molluscs, presents the first opportunity for the development of annually resolved marine spatial networks directly analogous to the dendrochronological networks.

Long-lived bivalve species containing annually-formed growth increments, such as *G. glycymeris* and *A. islandica*, enable the generation of sclerochronologies that are powerful archives of past oceanographic variability. The application of growth increment width chronologies and the associated geochemical series derived from the absolutely-dated growth increments have enabled the reconstruction of a broad array of oceanographic parameters including SST's (Schöne et al., 2005; Reynolds et al., 2013), marine radiocarbon reservoir ages (Wanamaker et al., 2012); high latitude seawater density (Richardson et al., submitted) and coupled ocean atmosphere climate fluctuations (Helama et al., 2007; Black et al., 2014). Spatial correlations reported in these studies indicate that sclerochronological records contain the imprints of both local and regional scale climate variability, and it is therefore likely that spatial network techniques can be used with these series to enhance the reconstruction of large scale oceanographic variability (e.g. surface ocean circulation, AMOC).

Here we examine a suite of sclerochronologies spanning the coastal shelf seas of the western British Isles ranging from St. George's Channel in the Southern Irish Sea to the Tiree Passage in northwest Scotland (Fig. 1 and Table 1) and extending back to the 16th century. Whilst oceanographic variability across the coastal shelf seas of North West Europe is heterogeneous (associated with local hydrographic, topographic and bathymetric conditions), variability of the western British Isles is dominated by the northward transport of warm saline waters derived from the North Atlantic Current (Fig. 1; Holliday et al., 2015; Inall et al., 2009). Therefore, although these sites span some 500 km of coastline they represent a relatively unified oceanographic regime and thus provide an opportunity to assess the ability of sclerochronology-based marine spatial networks to reconstruct broad scale oceanographic variability.

## 2. Methods

The construction of a sclerochronological spatial network is a multi-step process that requires careful consideration at each stage. Fig. 2 provides a schematic of the work flow we followed in the generation of each of the composite series. It ranges from the selection of the individual chronologies, data screening (which incorporates the correlation analyses between the individual chronologies and the examination of the environmental sensitivity of each individual chronology), the application of spatial weighting (through generating local composites), through to the generation of the composite series and finally the calibration and verification process. In total we produced five composite series, one containing all eight individual chronologies and four containing individual chronologies that were found to be sensitive to the discrete target parameters (AMO, wNAO, CET and Northeast Atlantic SST's). We applied the same standardised methodology for the production of each of the composite series in order to provide a fair assessment of the potential of using these techniques for reconstructing broad scale climate variability.

### 2.1. Chronology selection

For the reconstruction of basin scale oceanographic variability, it would be advantageous to incorporate individual chronologies from the broadest possible array of environments spanning a significant interval of time. However, hitherto there are relatively few regions with a sufficient number of robustly constructed absolutely-dated individual chronologies to facilitate such a broad scale spatial network. The continental shelf of the western British Isles currently contains the highest density of absolutely-dated independently constructed sclerochronologies of any region in the global ocean (eight chronologies). The high density of records from this region coupled with the relatively well understood oceanographic regime makes this an ideal test bed for the application of spatial networking methods.

The individual chronologies examined in this study were independently constructed using annually-resolved growth increment widths from live and dead *A. islandica* and *G. glycymeris* shells collected at sites ranging from the St. George's Channel in the southern Irish Sea to Tiree Passage in northwest Scotland (Table 1 and Fig. 1). The eight chronologies contained in this region were however not evenly distributed. In total the St George's Channel site contains three *G. glycymeris* sclerochronologies (Richardson unpublished; see supplementary information); the Isle of Man site contains two *G. glycymeris* (Brocas et al., 2013) and one *A. islandica* sclerochronology (Butler et al., 2010); Belfast Lough contains a single *A. islandica* sclerochronology (Ridgway et al., 2012; Román-González unpublished; see Supplementary information); and the Tiree Passage contains a single *G. glycymeris* sclerochronology (Reynolds et al., 2013; Fig. 2). The chronologies span a total period from CE 1516–2012 (Table 1).

The strength of the expressed population signal (EPS) of each of the chronologies was used to assess whether each of the individual chronologies should be incorporated into the spatial network. The EPS statistic is a measure of the degree to which the individual chronology represents the common population growth (Wigley et al., 1984). The degree of correlation between individual shell growth increment series and the associated sample depth (number of shells crossdated into the chronology in any given year) define the resulting strength of the EPS. Individual chronologies that contain a high sample depth (constructed using a large number of shells) and a high degree of correlation between the shell growth increment width series typically containing a high EPS statistic. Prior to the incorporation of the individual chronologies into the spatial network the EPS statistics of each of the chronologies were examined in order to assess the strength of their common growth signal. Series that contain an EPS >0.85 were deemed to have a significant common signal and therefore the chronology is deemed significantly robust.

Please cite this article as: Reynolds, D.J., et al., Reconstructing North Atlantic marine climate variability using an absolutely-dated sclerochronological network, Palaeogeogr. Palaeoclimatol. Palaeoecol. (2016), http://dx.doi.org/10.1016/j.palaeo.2016.08.006

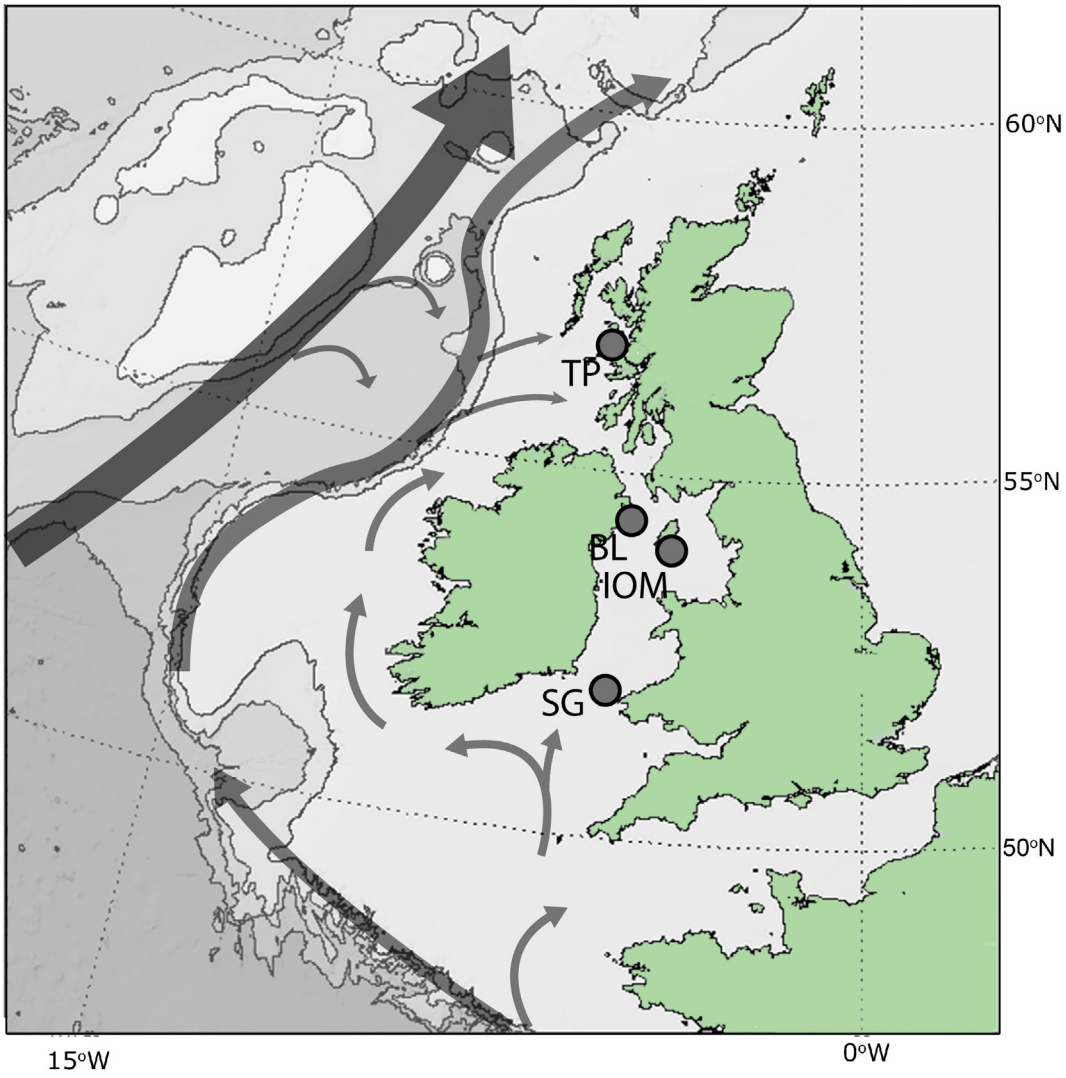


**Fig. 1.** Map showing the locations of the each of the sclerochronology sites (SG = St. George's Channel; IOM = Isle of Man; BL = Belfast Lough; and TP = Tiree Passage) along with the surface currents of the northeast Atlantic.

**Table 1**
Details of each of the chronologies considered for inclusion in the composite series. As well as the general sampling location water depth and species used for the individual chronology the duration of the chronology and associated expressed population statistics are provided (date provided in brackets denotes the calculation period). Chronologies with an EPS ≥ 0.85 are deemed robust.

| Individual chronology | Locality | Latitude and longitude | Species | Water depth (m) | Chronology period (years CE) | EPS | Published |
|---|---|---|---|---|---|---|---|
| Hart 7 | St George's Ch. | 51°58′51.97″N 5°53′49.95″W | *G. glycymeris* | 96 m | 1975–2001 | 0.86 (1975–2001) | Richardson unpublished data |
| Hart 8 | St George's Ch. | 52°1′44.93″N 5°45′6.48″W | *G. glycymeris* | 92 m | 1969–2001 | 0.83 (1969–2001) | Richardson unpublished data |
| Hart 67 | St George's Ch. | 51°57′14.56″N 5°47′18.00″W | *G. glycymeris* | 103 m | 1878–2001 | 0.82 (1950–2001) | Richardson unpublished data |
| IOM Neg | Isle of Man | 54°5′42.54″N 4°50′35.59″W | *A. islandica* | 35–70 m | 1516–2004 | >0.85 (1650–2004) | Butler et al. (2009) |
| IOM 97 | Isle of Man | 54°06.031′N 04°23,195′W | *G. glycymeris* | 35–40 m | 1930–1997 | 0.87 (1930–1997) | Brocas et al. (2013) |
| IOM 09 | Isle of Man | 53°59′32.40″N 4°39′17.27″W | *G. glycymeris* | 55–60 m | 1949–2006 | 0.94 (1949–2006) | Brocas et al. (2013) |
| TP | Tiree Passage | 56°37′47.33″N 6°24′15.86″W | *G. glycymeris* | 30–55 m | 1805–2010 | 0.85 (1850–2010) | Reynolds et al. (2013) |
| BL | Belfast Lough | 54°41′14.37″N 5°40′52.00″W | *A. islandica* | 20–30 m | 1839–2012 | 0.88 (1839–2012) | Ridgway et al. (2012) & Roman-Gonzalez unpublished data |

Please cite this article as: Reynolds, D.J., et al., Reconstructing North Atlantic marine climate variability using an absolutely-dated sclerochronological network, Palaeogeogr. Palaeoclimatol. Palaeoecol. (2016), http://dx.doi.org/10.1016/j.palaeo.2016.08.006

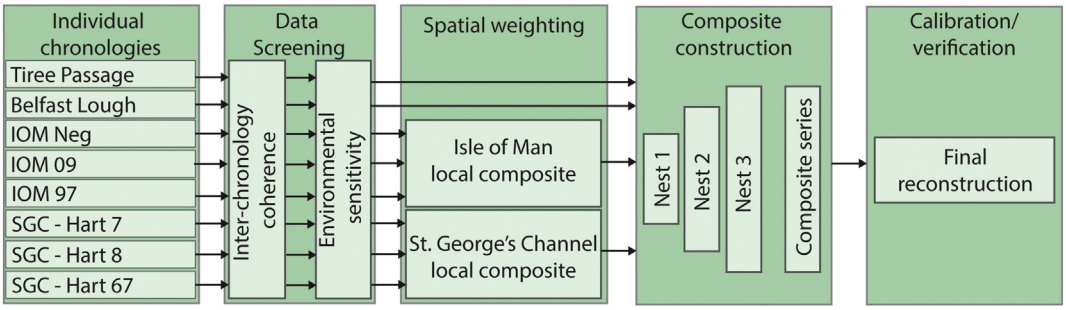


**Fig. 2.** Work flow schematic of the methods used to generate the climate reconstruction derived from the composite series. Arrows denote the workflow of the individual chronologies through the data screening process, spatial weighting (spatial weighting did not apply to the Belfast Lough and Tiree Passage chronologies) and into the construction of the composite series via three nests, Calibration verification techniques were then applied to the composite series to generate the final reconstruction. The length of the light green rectangles around Nests 1–3 indicates that each nest increases in temporal length due to the removal of shortest time series at each step. (For interpretation of the references to colour in this figure legend, the reader is referred to the web version of this article.)

### 2.2. Data screening

We applied a two-step data screening approach that incorporated the assessment of the strength of the inter-chronology correlations and the assessment of the sensitivity of each of the individual chronologies to a series of target environmental parameters. These steps are important as it is likely that each chronology contains subtly different environmental signals, due to the range of environments and water depths from which the shells were collected, and potential species-specific responses to environmental variability. Although compositing series across a large geographical area averages out purely local signals and strengthens the common regional signal it is important to avoid spurious interpretations of a climatological response derived from individual series that contain little or no coherence (Wilson et al., 2006). The inter-chronology coherence was assessed using a correlation matrix constructed using linear regression analyses between each of the individual chronologies over the single common period (1975–1990; Table 2).

To provide an assessment of the sensitivity of each individual chronology to the target environmental parameters we used linear correlation analyses, calculated between the individual chronologies and the seasonal mean (spring, summer, autumn and winter) AMO; (Trenberth and Shea, 2006) NAO; (Hurrell, 1995; Jones et al., 1997) CET; (Parker and Horton, 2005) and SSTs (using HadISST1 data; Rayner et al., 2003). Whilst the AMO, NAO, CET time series are established climatological records, the record of SSTs used here was a subset of the HadISST1 data (Rayner et al., 2003). We extracted SST data from a 10°x10° grid box (50–60°N 0–10°W) from the HadISST1 gridded dataset. The SST variability contained in this grid box is highly representative of the SST variability on the continental shelf surrounding the British Isles and in the wider northeast Atlantic region (Supplementary Fig. S1). The linear regression analyses were conducted over the period from 1950 to 2000.

We applied two approaches for the selection of the individual chronologies for the next stage of the composite construction. In the first approach all individual chronologies were utilised regardless of their correlation to the target environmental parameter. In the second approach only chronologies that showed either a significant positive or negative correlation ($P < 0.1$) to the target environmental parameter were selected.

### 2.3. Spatial weighting

Spatial weighting techniques were applied in order to mitigate the possibility of the over amplification of local signals caused by the heterogeneous nature of the distribution of the individual chronologies over the study area. For example, if a composite series were to be constructed using three individual chronologies from a single location and only one from another location, it is likely that the resulting composite record would be heavily biased towards variability at the location with more chronologies and not reflect the true common variability between the locations. In dendrochronological studies the application of spatial weighting techniques has been used in an attempt to mitigate these potential spatial biases through the generation of a local composite prior to the construction of the final composite series. In the above example these techniques would result in a local composite being constructed using the three individual chronologies from one location. This local composite would then be incorporated into the spatial network, along with the single individual chronology from the other location. The final composite, generated using the two locations, would therefore reflect a more robust balance of the variability between the two localities.

The application of such spatial weighting techniques, however, requires caution due to the realistic possibility that localised heterogeneity in the marine environment might cause further regional biases as a result of incorrect compositing of the series (e.g. Cunningham et al., 2013). Furthermore, as individual chronologies are constructed from different bivalve species, it is also necessary to consider potential differences in the species sensitivity to the target environmental parameters. Therefore, individual chronologies were only considered for spatial

**Table 2**
Pearson correlation matrix conducted between each of the individual chronologies. * Denotes significant correlations at $P < 0.1$ level. Distances between each of the sampling locations is given in the lower portion of the matrix. Distances calculated are the linear ground distance between each of the locations.

| Chronology | Hart 7 | Hart 8 | Hart 67 | IOM Neg | IOM 97 | IOM 09 | TP | BL |
|---|---|---|---|---|---|---|---|---|
| Hart 7 | | 0.101 | 0.000 | −0.472* | −0.185 | −0.311 | −0.220 | 0.113 |
| Hart 8 | 11 km | | −0.318 | −0.001 | 0.043 | −0.213 | 0.076 | 0.041 |
| Hart 67 | 8 km | 9 km | | −0.190 | 0.021 | −0.193 | −0.481* | −0.210 |
| IOM Neg | 245 km | 238 km | 246 km | | 0.079 | 0.499* | 0.681* | 0.064 |
| IOM 97 | 256 km | 246 km | 256 km | 30 km | | 0.462* | 0.238 | −0.069 |
| IOM 09 | 238 km | 231 km | 238 km | 17 km | 21 km | | 0.761* | −0.167 |
| TP | 518 km | 514 km | 522 km | 298 km | 310 km | 314 km | | 0.156 |
| BL | 301 km | 296 km | 304 km | 85 km | 160 km | 103 km | 220 km | |

Please cite this article as: Reynolds, D.J., et al., Reconstructing North Atlantic marine climate variability using an absolutely-dated sclerochronological network, Palaeogeogr. Palaeoclimatol. Palaeoecol. (2016), http://dx.doi.org/10.1016/j.palaeo.2016.08.006

weighting providing they had met the individual chronology selection criteria as part of the data screening step. As these criteria did not necessarily require the individual chronologies to have the same environmental response (e.g. they could have significant positive or negative coherence to the target parameter) the application of simple arithmetic mean to generate the local composite was deemed inappropriate. Therefore PCA techniques were used to construct the local composite series (Cunningham et al., 2013). The PCA was conducted using SBSS v20.

The spatial distribution of the chronologies examined here required the generation of two local composite series, one each from the St. George's Channel and the Isle of Man, as these localities each contained three individual chronologies. Local composites were not required from the Tiree Passage and Belfast Lough sites as only a single individual chronology was used from each of these locations. PCA was used to generate the local composites as it identifies and extracts the common variance from the suite of selected individual chronologies generating a series of principal components (PCs) that each contain estimates of the proportion of common variance across the individual chronologies, with PC1 containing the greatest degree of common variance across the series.

### 2.4. Network construction

For the construction of the final composite series, PCA was conducted between the selected individual chronologies and local composites in order to generate a single time series reflecting the common growth across the study region. The Eigenvalues and percentage variance statistics of each of the PCs generated by the PCA were used to assess the significance of the PCs. The primary PCs that contained an Eigenvalue >1 were deemed robust. One of the constraints of using the PCA approach to construct the composite series is that it requires all individual chronologies, or local composite series incorporated into the analyses, to be the same length, i.e. to cover a common time window. In order to overcome this problem a nested approach was taken in which once the primary PCA was completed, generating the primary nest, the PCA was repeated a second time with the shortest individual chronology, or local composite series, removed to generate a secondary nest (Wilson et al., 2010; Cunningham et al., 2013). This process was then repeated sequentially removing the next shortest series producing a tertiary nest. The secondary and tertiary nests were then spliced (with no overlap) onto the primary PC allowing for the generation of the composite series that span the period from 1805 to 2010. The nests were spliced together rather than averaged in order to mitigate the possibility of reintroducing bias towards localities incorporated into multiple nests. As each of the nests contains a different number of individual chronologies or local composites, it is important to assess the degree of coherence between the nests and to quantify the degree of uncertainty that is generated by the reduction in sample depth. We assessed these uncertainties by evaluating the degree of coherence and the mean squared error between each of the nests over the calibration period (1975–2000).

### 2.5. Environmental analysis

Prior to the application of the calibration and verification techniques each of the composite series were correlated against the mean annual and mean seasonal (spring, summer, autumn and winter) environmental time series (AMO, NAO, CET and SSTs) in order to define the seasonal sensitivity of the composite series. These initial correlations were calculated over the period 1950–2000 (Fig. 6). The spatial extent of the correlations were determined using spatial correlation analyses conducted between the composites and North Atlantic SSTs, air temperatures and sea level pressure (calculated over the same 1950–2000 period) using the KNMI climate explorer facility (Fig. 7; http://climexp.knmi.nl; Trouet and Van Oldenborgh, 2013). The spatial correlations were recalculated using linear detrended data to remove the influence of long-term trends.

We applied the standard dendrochronological calibration and verification techniques to calibrate each of the composite series against the target parameters and to provide a quantitative assessment of the skill of each reconstruction. Linear regression analyses were used to empirically derive a transfer function to calibrate each of the composite series to the target parameters (AMO, SSTs, wNAO, CET). The calibration linear regression analyses (Fig. 8) were performed over the calibration period. As each composite series was constructed from three nests we independently assessed the strength of the correlation coefficient between the target time series and each of the nests to assess the potential change in correlation due to a reduction in sample depth between the nests (Fig. 9). These correlations were calculated over the calibration period. Given that climatological time series typically contain high levels of autocorrelation we tested the significance of each correlation using a phase-randomizing bootstrapping technique with 1000 Monte Carlo runs (Ebisuzaki, 1997), and adjusted the corresponding probability accordingly.

Reduction of error (RE) and coefficient of efficiency (CE) statistics were used to assess the skill of the reconstructions over independent calibration and verification periods. Palaeoclimate reconstructions are deemed to contain a significant skill at reconstructing the target parameter if both the RE and CE statistics are significant (>0) and the reconstruction contains a significant percentage variance ($R^2$) over both the calibration and verification intervals (North et al., 2000). The CE statistic provides a robust independent assessment of the skill of the reconstruction as it is calculated using the proportion of the instrumental data that was not used in the initial calibration of the composite series.

Following the initial calibration of the composite series to the target parameters over the calibration period we calculated the $R^2$, RE and CE statistics over two independent 25 year time windows (Table 5). The RE and CE assessment of skill is based on the ability of the calibrated composite series to detect a shift in the mean of the target parameter between the two calculation periods (North et al., 2000). This approach was taken as climate reconstructions derived from detrended growth increment width series are notoriously bad at reconstructing low frequency climate variability (e.g. Reynolds et al., 2013). In addition we assessed the preservation of low frequency variability in the composite series by comparing the linear trends over the 20th century and the multi-taper method (MTM) spectral analyses of the composite series and the target instrumental series. The MTM spectral analyses were conducted using the K-Spectra application.

## 3. Results

### 3.1. Chronology selection

All eight individual chronologies analysed contained an EPS of ≥0.85 over a proportion of the time period covered by the chronology and a mean EPS ≥0.80 and are therefore included in our analyses (Table 1). For the previously unpublished chronologies (Hart 7, Hart 8, Hart 67 and Belfast Lough) running EPS statistics are provided in the supplementary information (Figs. S4–7). For more detailed descriptions of the Tiree Passage *G. glycymeris* see Reynolds et al. (2013), the Isle of Man *G. glycymeris* chronologies see Brocas et al. (2013) and the Isle of Man *A. islandica* chronology see Butler et al. (2009). Prior to 1950 the EPS of the Hart 8 chronology becomes highly variable and so this portion of the record was not incorporated into the network analyses (Fig. S5). All individual chronologies were truncated for intervals for which the EPS was <0.80. The strong EPS statistics of the eight chronologies indicates that these series could reliably be used for the construction of a sclerochronological spatial network.

Please cite this article as: Reynolds, D.J., et al., Reconstructing North Atlantic marine climate variability using an absolutely-dated sclerochronological network, Palaeogeogr. Palaeoclimatol. Palaeoecol. (2016), http://dx.doi.org/10.1016/j.palaeo.2016.08.006

### 3.2. Data screening

#### 3.2.1. Inter-chronology coherence

Pearson correlation analyses (Table 2) conducted between each of the individual chronologies over the single common period (1975–1990) indicated a broad range of correlations. The strongest correlations were identified between the Isle of Man (IOM_09) and Tiree Passage *G. glycymeris* chronologies ($R = 0.761$, $P < 0.01$) and the Isle of Man *A. islandica* and Tiree Passage *G. glycymeris* chronologies ($R = 0.681$, $P < 0.01$) indicating that, despite the ca. 300 km distance between these locations, the *A. islandica* and *G. glycymeris* populations are forming their growth increments in relative synchrony. The *G. glycymeris* chronologies from St. George's Channel exhibit significant negative coherence with each other (Hart 8 and Hart 67 chronologies; $R = -0.318$, $P < 0.1$) whilst exhibiting negative correlations with the Isle of Man *A. islandica* ($R = -0.472$; $P < 0.1$), and the Tiree Passage *G. glycymeris* chronology ($R = -0.481$ $P < 0.1$). The Belfast Lough chronology exhibits no significant correlation with any of the individual chronologies.

#### 3.2.2. Environmental sensitivity

Pearson correlation coefficients calculated between each of the individual chronologies and mean annual and seasonal (spring, summer, autumn and winter) target climate indices (AMO, wNAO, CET and SSTs) indicated that the chronologies show somewhat varied relationships with these environmental parameters (Fig. 3). The Isle of Man (IOM 09 and IOM 97) and Tiree Passage *G. glycymeris* chronologies, show significant positive correlations ($P < 0.1$) with the AMO, SSTs and CETs and wNAO (Fig. 4). The Hart 8 and Hart 67 chronologies show significant positive correlation to winter CETs, whilst the Hart 7 chronology show a significant negative correlation to the NAO. The Hart 67 chronology exhibits significant positive correlations with the AMO ($R = 0.56$, $P < 0.1$). The linear regression analyses indicated that the IOM Neg chronology is significantly sensitive to SSTs and CETs. The lack of sensitivity of the Belfast Lough chronology, and the variable nature of the correlations to the target environmental time series, may be caused by a number of factors including for example the interference of local environmental variability, such as freshwater run off or a stratified water column creating a buffer from SST and atmospheric variability, complexity in the signal because of sensitivity to multiple environmental parameters, variability in the factors that define the climate indices that is not reflected locally, or the fact that these series are just not sensitive to some broad scale climate drivers.

### 3.3. Composite construction

In total five composite series were constructed, one containing all eight individual chronologies and four containing only the chronologies that demonstrated a significant ($P < 0.1$) correlation to the selected environmental parameter. Table 3 outlines which individual chronologies were incorporated into each composite and whether they were incorporated as part of a local composite series prior to the construction of the final composite series. Each composite was assigned an acronym that denotes the individual chronology selection criteria applied. The All Comp. composite contains all of the individual chronologies, whilst the AMO-SC, CET-SC, SST-SC and wNAO-SC composites contain only individual chronologies that contain a significant ($P < 0.1$) correlation with the corresponding target parameter (Table 3). The PC 1 produced in the generation of each of the five composite series contained

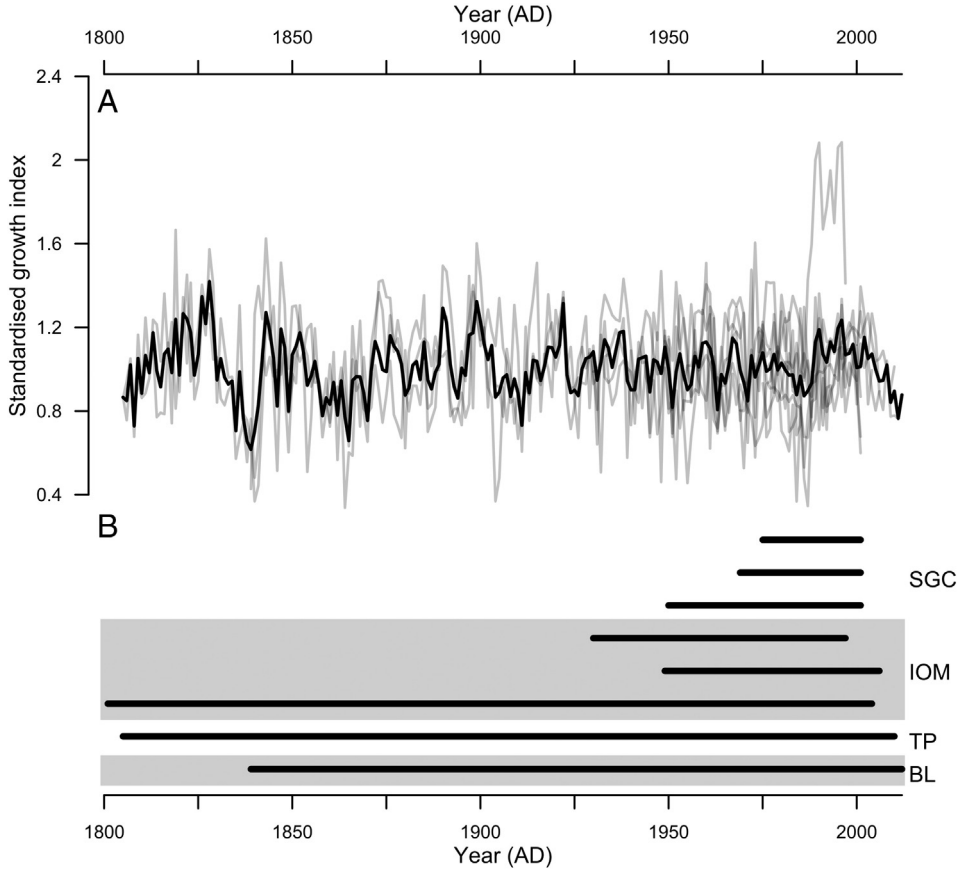


**Fig. 3.** A) Standardised growth increment widths from the eight chronologies (grey line) and a composite average (black line). B) Relative temporal alignment of each of the chronologies (represented by the black bars), SG = St. George's Channel; IOM = Isle of Man; BL = Belfast Lough; TP = Tiree Passage.

Please cite this article as: Reynolds, D.J., et al., Reconstructing North Atlantic marine climate variability using an absolutely-dated sclerochronological network, Palaeogeogr. Palaeoclimatol. Palaeoecol. (2016), http://dx.doi.org/10.1016/j.palaeo.2016.08.006

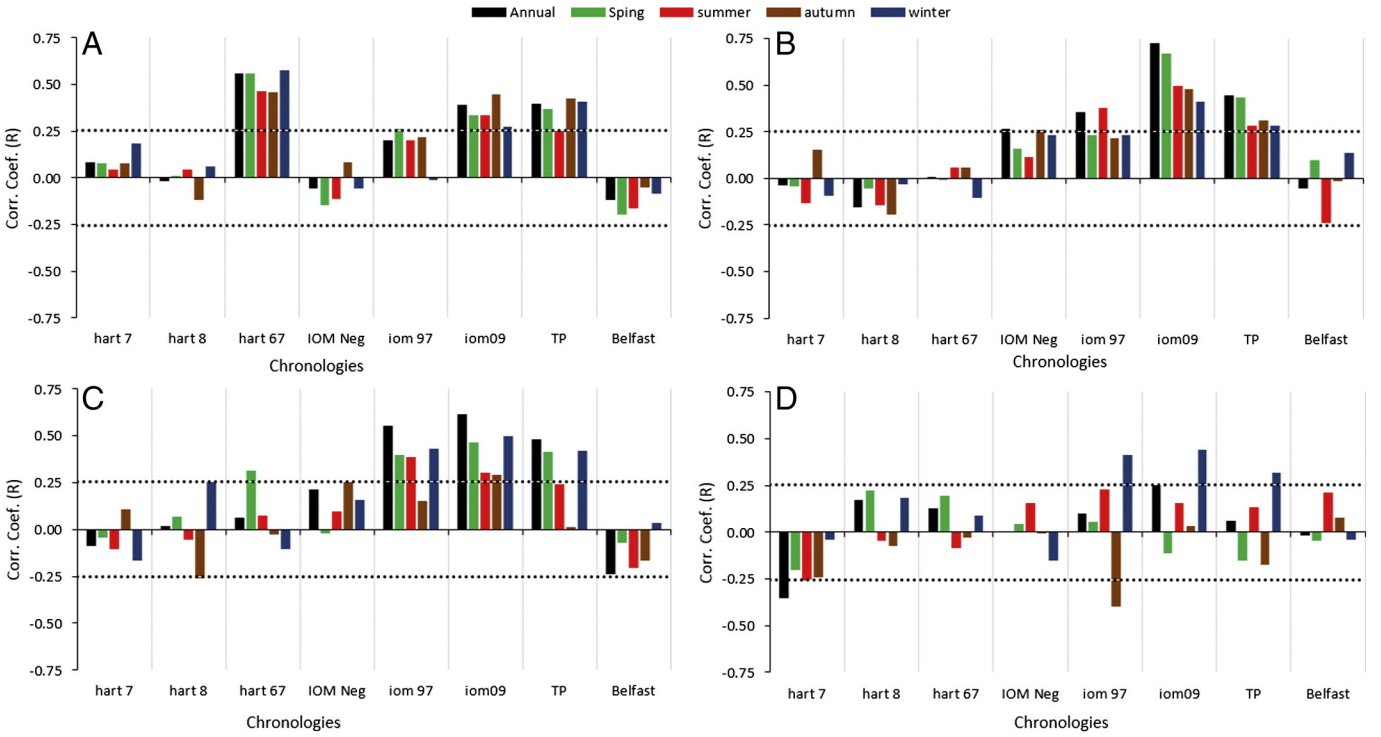


**Fig. 4.** Pearson correlation coefficients calculated between the individual chronologies and mean annual (black bars) and seasonal (spring, summer, autumn and winter, green, red, brown and blue bars respectively) A) Atlantic Multidecadal Oscillation (AMO); B) Northeast Atlantic sea surface temperatures (SSTs); C) Central England Temperature (CET) series; and D) the North Atlantic Oscillation (NAO). Correlations calculated over the period 1975–1990. Dotted black lines represent the 90% significance level. (For interpretation of the references to colour in this figure legend, the reader is referred to the web version of this article.)

significant eigenvalues (>1; Table 4). Each of these PC's, which are the primary nest of each of the five composite series, explained between 31% and 74% of the variance across the incorporated individual chronologies (mean percentage variance across the five composites of 51%; Table 4). The significant eigenvalues and high percentage variance scores suggests that PCA analyses can be used to define and extract the common variance in the individual chronologies.

Each of the PCA's conducted in the generation of the secondary and tertiary nests also resulted in the generation PCs containing significant eigenvalues. Examination of the percentage variance ($R^2$) and mean squared error (MSE) calculated between each of the nests used to construct the composite series indicates that, despite the reduction in the number of individual chronologies between each nest, each of the nests are highly correlated ($R^2 = 0.91$; $P < 0.001$). Due to this high level of coherence the associated MSE (0.12) equates to only 12% of the composite series standard deviation. Given the low MSE scores and the high correlation between the nests, the final composites were constructed by splicing the nests together with zero overlap.

### 3.4. Environmental analyses

Initial correlation analyses, calculated over the period from 1950 to 2000, indicated that all five composites, All Comp., SST-SC, CET-SC, AMO-SC and wNAO-SC, contained significant positive correlations against the corresponding target environmental time series ($P < 0.05$; Fig. 6 and Table 5). The spatial correlation analyses indicated that these correlations, whilst most strongly evident over the British Isles, extend over a significant proportion of the north east Atlantic region (Fig. 7). The spatial correlations calculated between the All Comp., SST-SC and AMO-SC against the HsdISST1 SST dataset (Rayner et al., 2003) indicated significant positive correlations propagating along the trajectory of the North Atlantic current and across the wider northwest European continental shelf into the Norwegian and Baltic Seas. The correlations with the HadCRU T4 air temperature index (Morice et al., 2012a,b) similarly centred on the British Isles, however, also follows the south west/north east pattern coincident with the prevailing surface air flow patterns. The spatial correlation patterns between the All Comp.

**Table 3**
Overview of which individual chronologies were incorporated into each of the composite series. The acronyms used for each of the composites are given in brackets. Individual chronology names followed by – SGCC or – IOMC indicates they were used to construct a local composite from either St. George's Channel or the Isle of Man respectfully prior to the construction of the final composite series.

| All series composite (All Comp.) | AMO composite (AMO-SC) | CET composite (CET-SC) | SST composite (SST-SC) | wNAO composite (wNAO-SC) |
|---|---|---|---|---|
| Hart 7 - SGCC | Hart 67 | Hart 8 - SGCC | IOM Neg - IOMC | Hart 7 - SGCC |
| Hart 8 - SGCC | IOM 97 - IOMC | Hart 67 - SGCC | IOM 97 - IOMC | IOM 97 - IOMC |
| Hart 67 - SGCC | IOM 09 - IOMC | IOM Neg - IOMC | IOM 09 - IOMC | IOM 09 - IOMC |
| IOM Neg - IOMC | TP | IOM 97 - IOMC | TP | TP |
| IOM 97 - IOMC | | IOM 09 - IOMC | | |
| IOM 09 - IOMC | | TP | | |
| TP | | | | |
| BL | | | | |

Please cite this article as: Reynolds, D.J., et al., Reconstructing North Atlantic marine climate variability using an absolutely-dated sclerochronological network, Palaeogeogr. Palaeoclimatol. Palaeoecol. (2016), http://dx.doi.org/10.1016/j.palaeo.2016.08.006

**Table 4**
Results of the PCA generating the primary nest in each of the respective composites (using all of the chronologies and the using the screening methodology). – denotes the chronology was not used in the construction of the respective composite series.

| | All Comp. | AMO-SC | CET-SC | SST-SC | wNAO-SC |
|---|---|---|---|---|---|
| Eigen value | 1.22 | 1.09 | 2.03 | 1.50 | 1.47 |
| % of variance | 31% | 36% | 67% | 74% | 49% |
| Chronology weighting | | | | | |
| Hart 7 | 0.656 | | | | −0.140 |
| Hart 8 | 0.656 | | −0.225 | | |
| Hart 67 | 0.656 | 0.432 | −0.225 | | |
| IOM Neg | 0.677 | | 0.994 | 0.865 | |
| IOM 97 | 0.677 | 0.869 | 0.994 | 0.865 | 0.849 |
| IOM 09 | 0.677 | 0.869 | 0.994 | 0.865 | 0.849 |
| TP | 0.559 | 0.562 | 0.994 | 0.865 | 0.855 |
| BL | 0.459 | | | | |

and NAO-SC composites and sea level pressure (SLP; Trenberth and Paolino, 1980) over the North Atlantic region (wNAO indices are derived from SLP indices) shows a strong dipole with significant negative correlations over the subpolar region centred around Iceland and significant positive correlations across a band of the North Atlantic between ca. 30–40°N. This pattern is consistent to that of the dipole SLP pattern of the wNAO. Examination of the spatial correlation patterns derived from using linear detrended composite and instrumental time series indicates that the composite series are highly coherent with the target environmental time series at inter-annual to multi-decadal timescales (Fig. 7C, F, I and L). These results suggest that low frequency variability, and autocorrelation, account for only a small degree of the covariance between the composite series and the target environmental variables. These primary results indicated that the composite series contained significant sensitivity to the target parameters and therefore each of the composite series was calibrated to the respective instrumental time series.

*3.4.1. Calibration and verification*

Each of the composite series was calibrated against the instrumental time series using linear regression analyses over the calibration period (Fig. 8). Table 2 provides all the calibration and verification statistics. The strength of the regression analyses varied between $R^2 = 0.04$ (All Comp. versus wNAO) and $R^2 = 0.45$ (CET-SC versus CET). However, the composite series consistently explained high levels of variance ($R^2 = 0.25$–$0.49$) in those time series that indicated temperature variability (AMO, CET and SSTs). The replication of these analyses using each of the nests used to construct each composite found that, despite the associated reduction in sample depth within the secondary and tertiary nests, the variance explained by the linear regression was broadly stable between each of the nests over the calibration period (Fig. 9). The RE statistics calculated over the calibration period indicate that all five composites contained significant skill (RE > 0) at reconstructing the target environmental parameters (Table 5). However, examination of the CE statistics, calculated between the calibrated composite series and the target parameters over the independent time interval (1950–1974), indicated that only the All Comp./SST-SC based reconstructions of SSTs and the wNAO-SC based reconstruction of the wNAO contained significant skill (CE > 0) over the verification period (1950–1974; Table 5). Examination of the linear trends in the instrumental datasets and the composite series highlights that whilst all four instrumental time series contain long-term linear trends, the composite series contain no significant linear trend over the 20th century (Fig. 10). The removal of these linear trends from the instrumental time series however, highlights the coherence of the composite series and target environmental time series at mid to high frequencies (inter-annual to multi-decadal). The MTM spectral analyses highlighted that whilst the composite series contain significant variability at multi-decadal periodicities none show any significant variability at low frequencies (lower than ca. 50 year periodicity; Fig. S8). In contrast however, the MTM spectral analyses of the instrumental time series indicates significant variability across all timeframes up to multi-centennial in scale (Fig. S8).

## 4. Discussion

Several recent papers have demonstrated that growth increment width sclerochronologies can provide robustly calibrated absolutely-dated and annually resolved reconstructions of past marine variability (e.g. Reynolds et al., 2013; Brocas et al., 2013; Black et al., 2014). The environmental signal contained in these reconstructions comprises some combination of local and regional scale variability dictated by the local hydrographic setting and the sensitivity of the species growth to environmental forcings (Wilson et al., 2010; Cunningham et al., 2013). The presence of a regional signal in the composite series we examine

**Table 5**
Calibration and verification statistics calculated between the composites constructed containing all of the individual chronologies (All Comp.) and the chronologies sensitive to the four target environmental parameters (mean autumn AMO [AMO-SC], mean annual SSTs [SST-SC], mean annual CETs [CET-SC] and wNAO [wNAO-SC]). The table outlines the Pearson correlation (R), percentage variance ($R^2$), and reduction of error (RE) and coefficient of efficiency (CE) statistics calculated over independent calibration and verification periods. * denotes a significant (>0) RE/CE statistic.

| | | All composite | | AMO-SC | | | | |
|---|---|---|---|---|---|---|---|---|
| AMO | | R | $R^2$ | R | $R^2$ | | All Comp. | AMO-SC |
| Calibration period | 1975–2000 | 0.62 | 0.39 | 0.70 | 0.49 | RE | 0.35* | 0.47* |
| Verification period | 1950–1974 | 0.10 | 0.01 | 0.06 | 0.00 | CE | −0.22 | −0.21 |
| | | All composite | | SST-SC | | | | |
| SSTs | | R | $R^2$ | R | $R^2$ | | All Comp. | SST-SC |
| Calibration period | 1975–2000 | 0.55 | 0.30 | 0.64 | 0.41 | RE | 0.30* | 0.41* |
| Verification period | 1950–1974 | 0.57 | 0.33 | 0.47 | 0.22 | CE | 0.22* | 0.33* |
| | | All composite | | CET-SC | | | | |
| CET | | R | $R^2$ | R | $R^2$ | | All Comp. | CET-SC |
| Calibration period | 1975–2000 | 0.50 | 0.25 | 0.54 | 0.29 | RE | 0.25* | 0.29* |
| Verification period | 1950–1974 | 0.60 | 0.36 | 0.47 | 0.22 | CE | −0.39 | 0.20* |
| | | All composite | | wNAO-SC | | | | |
| wNAO | | R | $R^2$ | R | $R^2$ | | All Comp. | wNAO-SC |
| Calibration period | 1975–2000 | 0.20 | 0.04 | 0.47 | 0.22 | RE | 0.04* | 0.22* |
| Verification period | 1950–1974 | 0.57 | 0.32 | 0.57 | 0.33 | CE | −0.04 | 0.25* |

Please cite this article as: Reynolds, D.J., et al., Reconstructing North Atlantic marine climate variability using an absolutely-dated sclerochronological network, Palaeogeogr. Palaeoclimatol. Palaeoecol. (2016), http://dx.doi.org/10.1016/j.palaeo.2016.08.006

supports evidence derived from the analyses of multiple geoduck chronologies (Black et al., 2009), otolith chronologies (Matta et al., 2016; Black et al., 2011) and cross-species otolith, molluscan and tree growth increment analyses (Black, 2009; Black et al., 2008) that sclerochronological networks contain coherent growth signals even if the individual chronologies they contain are separated by large distances. This demonstrates that spatial networking techniques similar to those applied to dendrochronological records (Wilson et al., 2010) can also be used with shell-based chronologies to enhance the reconstruction of large scale marine climate variability.

Oceanographic variability on the coastal shelf seas of the western British Isles, whilst locally heterogeneous, is fundamentally driven by the wider North Atlantic system. This region therefore provides an optimal test bed for the assessment of the use of spatial networking techniques with shell-based chronologies. The eight chronologies used here, spanning the geographical area from St. Georges Channel to northwest Scotland, exhibit a wide range of inter-correlations from significantly negative ($R = -0.47$) to significantly positive ($R = 0.76$), over the single common period (1975–1990, Table 2), indicating a degree of synchronous growth that is likely driven by a common environmental forcing. However, the presence of both positive and negative correlations between the chronologies indicates either that the sites are hydrographically distinct or that the populations differ in their response to the same environmental forcing because of differing biological response or the influence of local environmental factors (Witbaard et al., 2003). The Pearson correlations calculated between the individual chronologies and the target climate indices (Fig. 4) demonstrate that the individual chronologies contain differing levels of environmental coherence. The Isle of Man and Tiree Passage *G. glycymeris* chronologies exhibit significant strong positive correlations with northeast Atlantic SST and CET variability, whilst the *G. glycymeris* chronologies from St. George's Channel exhibit both positive correlations with CET and negative correlations with northeast Atlantic SSTs. The Belfast Lough *A. islandica* chronology exhibits no significant correlation to any of the target indices (Fig. 4). The levels of correlation identified are consistent with those identified during the calibration of the original series (Butler et al., 2010; Brocas et al., 2013; Reynolds et al., 2013). These data are, however, insufficient to determine whether the differences in correlation indicate differences in site-specific species climatic sensitivities or in local climatic conditions.

Despite the broad spectrum of inter-chronology correlations and individual chronology sensitivities to the target environmental time series, the PCA successfully extracts PCs with Eigenvalue >1(Table 4). The generation of robust PCs indicates that it is possible to extract a single robust time series that contains variability that is likely driven by a common environmental forcing. Furthermore, the correlation coefficients between nests used to extend the composites back through time indicate that the common signal identified between the individual chronologies appears to be robust irrespective of the number of chronologies incorporated into the PCA (Fig. 5). This conclusion is further supported by the consistent levels of correlation identified between each of the nests and the target environmental time series (Fig. 9).

The temporal and spatial correlation analyses (Figs. 6, 7 and 8) show that the composite series are highly sensitive to mean annual and seasonal AMO, SSTs, CET and wNAO variability in the northeast Atlantic and European region. The strength of the correlation between the composite records and the northeast Atlantic SSTs ($R = 0.61$ 1950–2000) are consistent with the correlations calculated between the individual *G. glycymeris* chronologies from both the Isle of Man and Tiree Passage correlated against local instrumental SSTs over a comparable timeframe ($R = 0.62$ 1949–2006 (Brocas et al., 2013); and $R = 0.74$ 1954–2007 (Reynolds et al., 2013)). Whilst the SST-SC composite is heavily weighted by both the Isle of Man and Tiree Passage *G. glycymeris* individual chronologies, the All Comp. series attains comparable levels of correlation ($R = 0.51$, 1950–2000) despite containing series that individually show less sensitivity to the target parameter. The split calibration

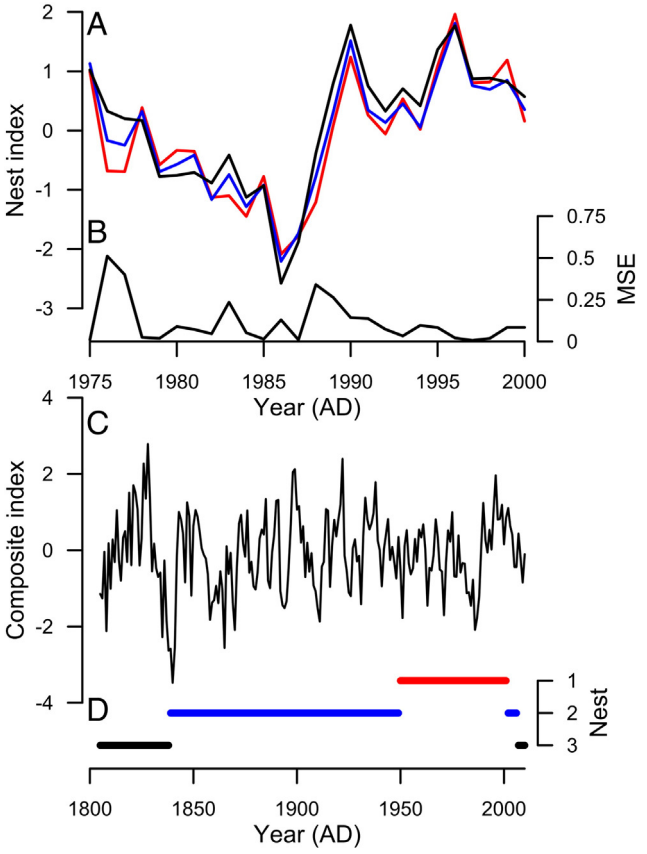


**Fig. 5.** A) Comparison between the primary (red line), secondary (blue line) and tertiary (black line) nests used to construct the composite series using all of the individual chronologies. B) Plot of the associated mean of the mean squared errors (MSE) calculated between each of the nests. C) The composite series and D) shows the position of the primary nest (red line; 1950–2001), secondary nest (blue line; 2002–2006 and 1839–1949) and tertiary nest (black line; 2007–2010 and 1805–1838). (For interpretation of the references to colour in this figure legend, the reader is referred to the web version of this article.)

verification approach shows that the calibrated All Comp./SST-SC and NAO-SC based reconstructions of SSTs and wNAO respectively contained significant skill at multi-decadal timescales (<50 year periodicity). Given the consistent high $R^2$ (0.43 and 0.37 over the calibration and verification periods respectively; Table 5) and the stable RE and CE values ($RE = 0.43$, $CE = 0.33$) the SST-SC based reconstruction of northeast Atlantic SSTs (Fig. 11) therefore presents the most skilful of the five composite based reconstructions and presents a reliable reconstruction of past multi-decadal scale SST variability in the northeast Atlantic region.

The spatial patterns of these correlations are consistent with the paradigm of the coupled ocean-atmosphere North Atlantic system and provide the potential to infer insights into the role of the North Atlantic system in driving European climate variability.

The northward transport of heat through the surface components of the AMOC influences the air-sea heat flux, most notably during the winter months (Frankignoul et al., 1998), acting as "bottom up" forcing (Tandon and Kushner, 2015) whereby the increase (reduction) in heat transported through the AMOC leads to a net warming (cooling) of SSTs and air temperatures across the European region. Such changes in the strength of the AMOC are hypothesised to be a significant contributing factor to the MCA-LIA transition (Lund et al., 2006; Trouet et al., 2012; Wanamaker et al., 2012). Conversely, variability in the atmospheric system driven by exogenic (solar) and endogenic (volcanic and anthropogenic) forcings as well as atmospheric blocking patterns (wNAO) act as "top down" drivers of Atlantic SSTs and, through feedback mechanisms, AMOC transport (Robock, 2000; Steinhilber et al.,

Please cite this article as: Reynolds, D.J., et al., Reconstructing North Atlantic marine climate variability using an absolutely-dated sclerochronological network, Palaeogeogr. Palaeoclimatol. Palaeoecol. (2016), http://dx.doi.org/10.1016/j.palaeo.2016.08.006

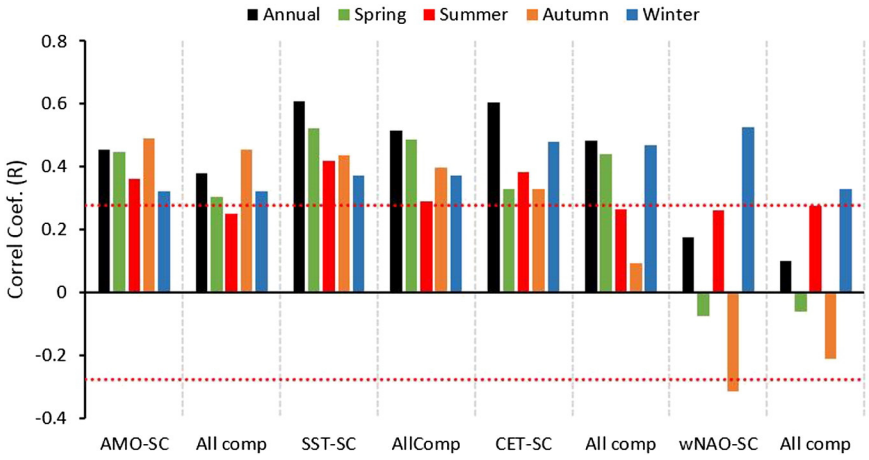


**Fig. 6.** Comparison between the Pearson correlation coefficients (R) calculated between the mean annual and seasonal AMO, CET, SST and NAO instrumental data and composite growth increment series constructed using the primary principal component of all the individual chronologies and those that only show a significant correlation with the target parameter (AMO, CET, SST and NAO weighted). The red dotted horizontal lines show the 95% significance level. Correlations calculated over the period from CE 1950-2000.(For interpretation of the references to colour in this figure legend, the reader is referred to the web version of this article.)

2009; Lockwood et al., 2011; Tandon and Kushner, 2015). The significant positive spatial correlations identified between the composite series and SSTs along the northeast Atlantic component of the North Atlantic Current and adjacent coastal currents, air temperatures centrally over the UK and the prevailing south-westerly wind direction, and the dipole in correlations with SLPs, coherent with the wNAO dipole

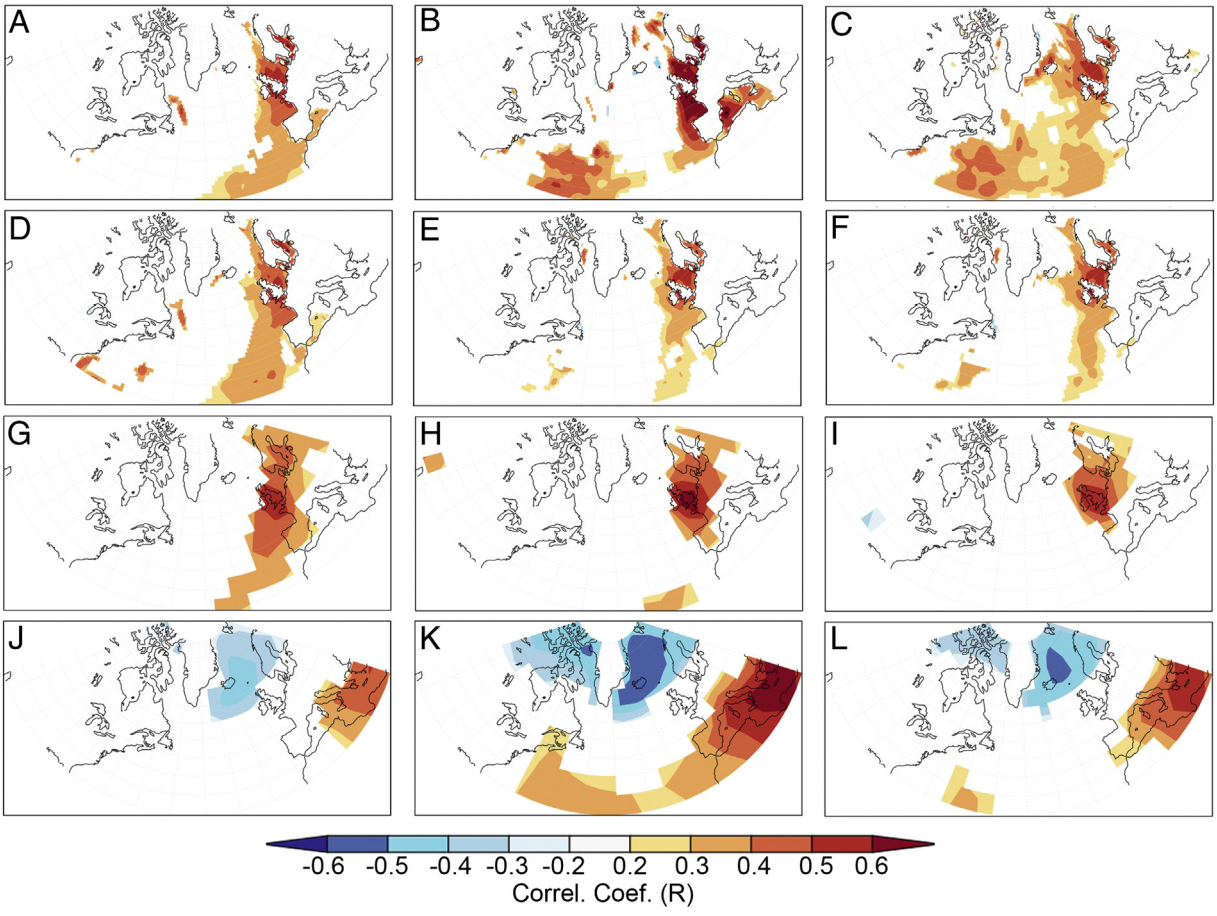


**Fig. 7.** Comparison between the spatial correlations calculated between the five composite series and the target environmental parameters. All correlations were calculated over a single common time window common (1950–2000). A) All Comp. correlated against mean annual HadISST1; B) AMO-SC correlated against mean August to November HadISST1; D) All comp. correlated against mean annual HadISST1; E) SST-SC correlated against mean annual HadISST1; G) All comp. correlated against mean annual HadCRUT4 air temperatures; H) CET-SC correlated against mean annual HadCRUT4 air temperatures; J) All comp. correlated against winter sea level pressures; and K) wNAO-SC correlated against mean winter sea level pressures. Plots C, F I and L show the correlations between the linear detrended AMO-SC, SST-SC, CET-SC and wNAO-SC composite series and the corresponding linear detrended (C and F) HadISST1 SSTs; I) CRU T4 air temperatures; and L) SLPs (Trenberth and Paolino, 1980).

Please cite this article as: Reynolds, D.J., et al., Reconstructing North Atlantic marine climate variability using an absolutely-dated sclerochronological network, Palaeogeogr. Palaeoclimatol. Palaeoecol. (2016), http://dx.doi.org/10.1016/j.palaeo.2016.08.006

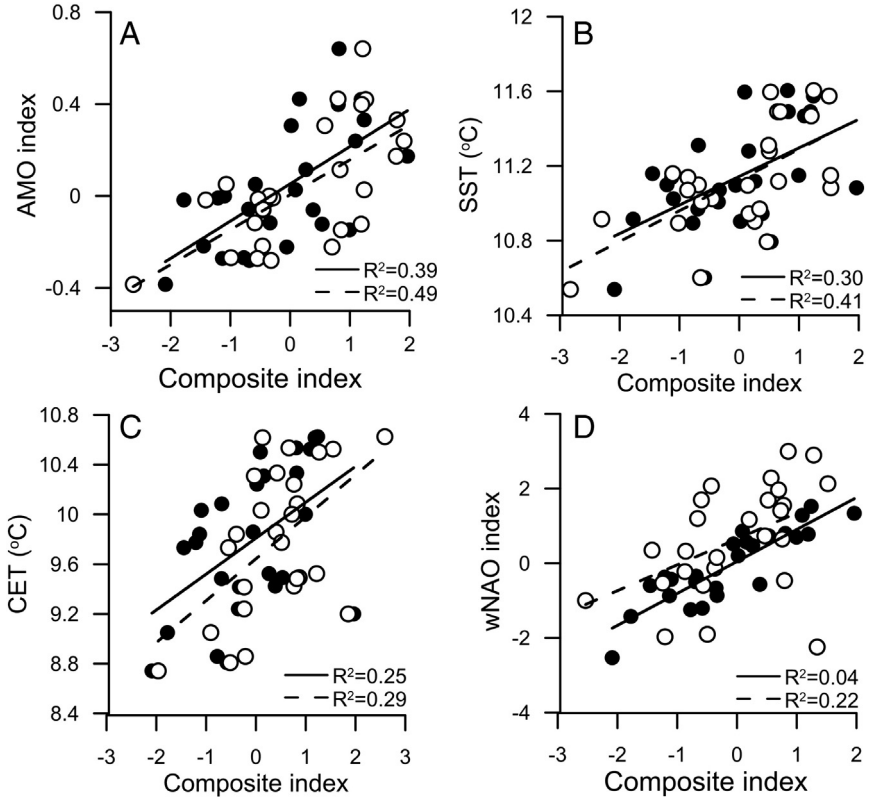


**Fig. 8.** Linear regression analysis between the composite constructed using all of the individual chronologies (black filled circles, and solid black regression line) and the chronologies sensitive to the target parameters (open black circles and dashed black regression line) and the four target parameters. A) Mean autumn AMO; B) annual mean SSTs; C) annual mean CETs; and D) wNAO. Regression analyses were conducted over the calibration period 1975–2000.

pressure gradient between Iceland and Gibraltar (Fig. 5), strongly indicate that the composite series is capturing broad scale climate variability in the North Atlantic system.

Previous studies have presented oceanographic reconstructions derived from growth increment width and geochemical series that show sensitivity to North Atlantic climate variability (Schöne et al., 2005; Reynolds et al., 2013; in review). The results presented here suggest that composite series derived from sclerochronological networks potentially contain comparable levels of skill with the best performing reconstructs of mean annual AMO, SSTs, CETs and the wNAO derived from individual chronologies (Table 6). This result supports the hypothesis that the combination of chronologies from across a range of habitats averages out the local environmental signals and preserves the broader scale climate signal (Wilson et al., 2010). Whilst the increase in skill is not consistent between all of the composites, the identification of highly significant correlations ($P < 0.05$) supports the potential of the combination of individual chronologies from environmentally sensitive areas can be used to reconstruct basin scale climate variability.

Given that the populations of the species considered here and their habitats are somewhat heterogeneous, site selection is often a compromise between identifying climatically sensitive locations and identifying sites that host abundant populations of the target bivalve species even if the sites themselves are not as climatically sensitive. The near comparable performance of the All Comp. and SST-SC composites at reconstructing northeast Atlantic SSTs indicates that, in future studies, the composites from multiple chronologies from locations known to contain abundant live and fossil samples, but that are less climatically sensitive, could be used to derive environmental reconstructions that are as good as or better than those obtained using individual chronologies from the most sensitive sites.

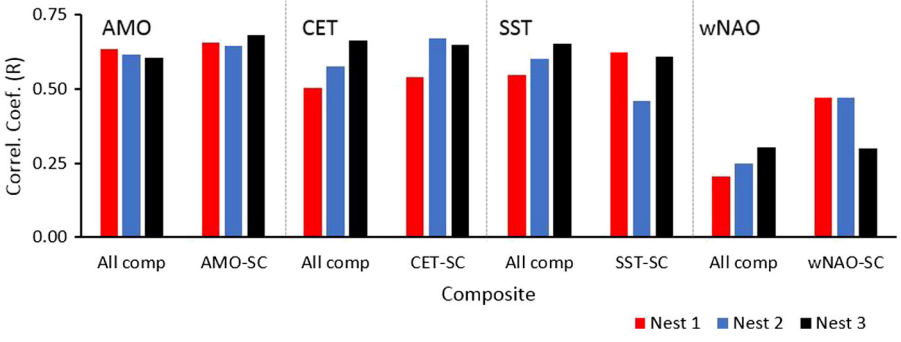


**Fig. 9.** Examination of the strength of the correlation between the target parameters (AMO, CET, SST and wNAO) and the individual nests used to construct each of the composite series. Red, blue and black bars indicate correlations calculated between the primary, secondary and tertiary nests and the target parameters respectfully. All correlations calculated over the calibration window (1975–2000). (For interpretation of the references to colour in this figure legend, the reader is referred to the web version of this article.)

Please cite this article as: Reynolds, D.J., et al., Reconstructing North Atlantic marine climate variability using an absolutely-dated sclerochronological network, Palaeogeogr. Palaeoclimatol. Palaeoecol. (2016), http://dx.doi.org/10.1016/j.palaeo.2016.08.006

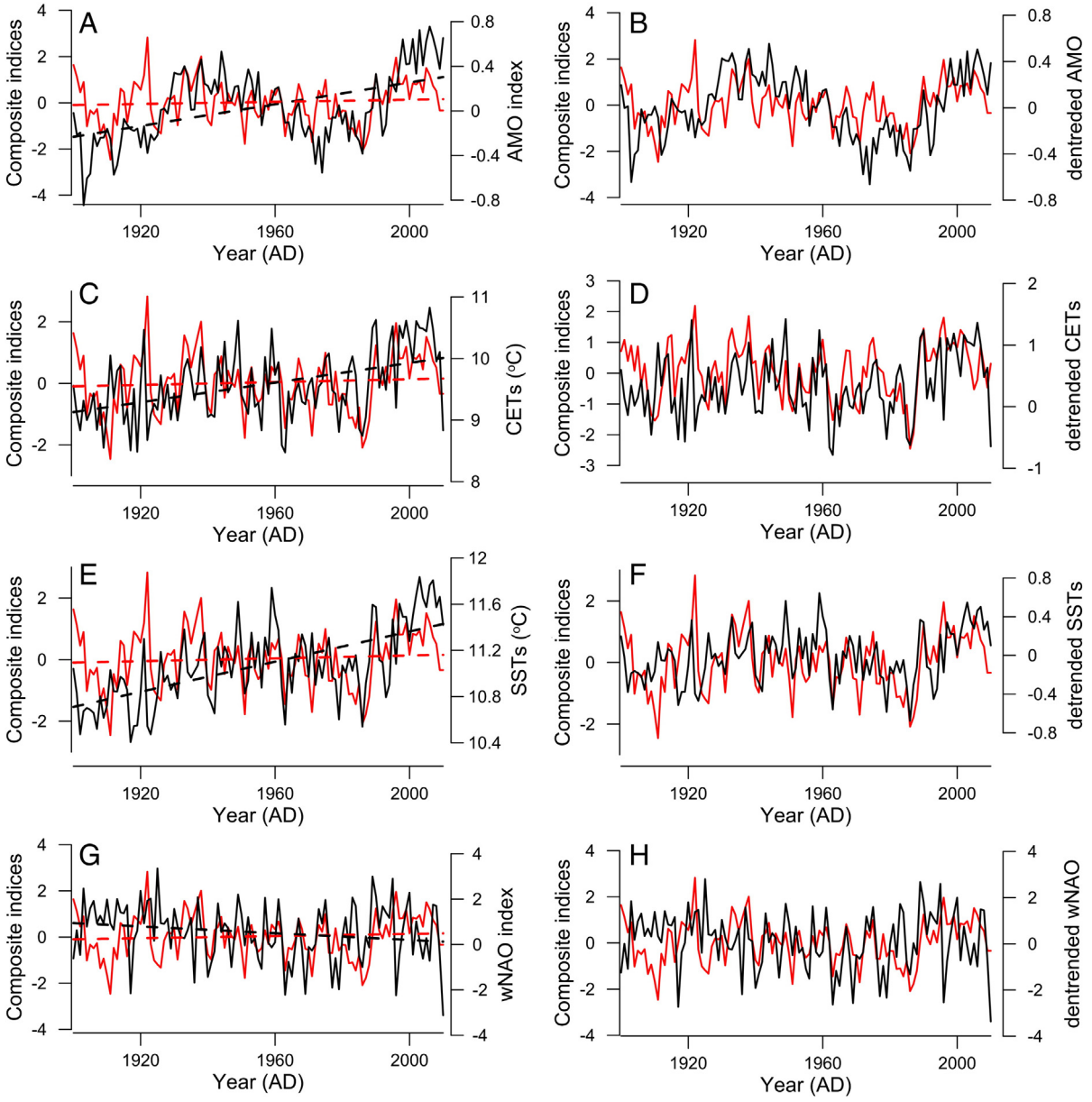


**Fig. 10.** Comparison between the composite series (red lines) and the target environmental datasets over the 20th century (black lines). Data displayed in panels (A), (C), (E) and (G) show the annually resolved AMO, CET, SST and wNAO records respectively. Composite and environmental data are fitted with linear trend lines shown in red and black dashed lines respectively. Panels (B), (D), (F) and (H) show the linear detrended AMO, CET, SST and wNAO records respectively (black lines) compared to the composite record (red lines). The composite record is not detrended in these panels. (For interpretation of the references to colour in this figure legend, the reader is referred to the web version of this article.)

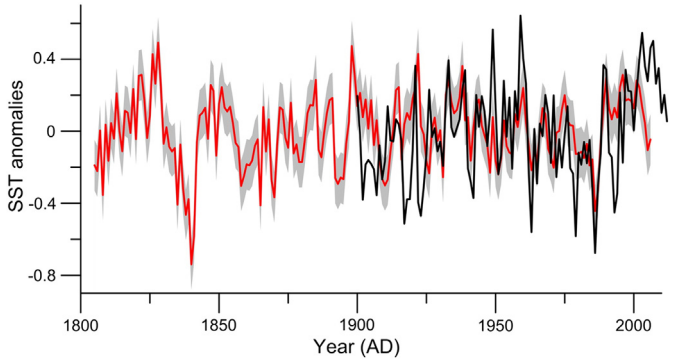


**Fig. 11.** Reconstructed high frequency (sub-centennial) mean annual SST anomalies based on the SST-SC series (red line). Black line shows linear detrended instrumental SST anomalies (HadISST1 50–60°N, 0–10°W). The shaded grey area denotes the two times mean squared error composite uncertainties. (For interpretation of the references to colour in this figure legend, the reader is referred to the web version of this article.)

Our results identified subtle differences in the level of environmental variance explained by the composite series that is likely related to the criteria used for the selection of the individual chronologies. For the AMO-SC, SST-SC and the CET-SC, where chronologies were selected

**Table 6**
Comparison between the Pearson correlations (R) calculated between the four target environmental parameters, the five composite series and the best performing individual chronologies. Mean correlation calculated between the four target parameters and the individual chronologies are also provided. Correlations calculated over the period from 1975 to 2000.

| Environmental target | Best individual chronology | Mean correlation with individual chronologies | All Comp. | SC composites |
|---|---|---|---|---|
| AMO | 0.58 (Hart 67) | 0.17 | 0.62 | 0.70 |
| CET | 0.62 (IOM09) | 0.20 | 0.50 | 0.54 |
| SSTs | 0.72 (IOM09) | 0.19 | 0.55 | 0.64 |
| wNAO | 0.40 (IOM09) | 0.15 | 0.20 | 0.47 |

Please cite this article as: Reynolds, D.J., et al., Reconstructing North Atlantic marine climate variability using an absolutely-dated sclerochronological network, Palaeogeogr. Palaeoclimatol. Palaeoecol. (2016), http://dx.doi.org/10.1016/j.palaeo.2016.08.006

for inclusion in the composite on the basis that they significantly correlated with the target climate indices, the correlation between the composite and the indices was increased (Fig. 4). However, the improvement was not consistent across the targets, being greatest for the wNAO (increase by 0.27 to $R = 0.47$; $P < 0.01$) and minimal for the AMO, SSTs and the CET (mean increase of 0.07). These results indicate the selection of individual chronologies that contain significant correlations to the target environmental time series does not greatly influence the reconstruction of temperature-based environmental parameters, but that it may help with the reconstruction of indices such as the wNAO that are derived from basin scale pressure gradients.

The significant calibration and verification statistics ($R^2$, RE and CE) calculated over the 25 year windows (1975–2000 and 1950–1974) indicates that the All Comp./SST-SC series contains significant skill at reconstructing multi-decadal SST in the western British Isles and Northeast Atlantic region (Fig. 11). However, the comparison of the linear trends in the instrumental and composite series over the entire 20th century indicate a lack of sensitivity to longer term low frequency variability. Examination of the MTM spectral plots (Fig. S8) indicates an absence of significant low frequency variability (periodicity lower than ca. 50 years) in the composite series whilst the instrumental data show significant variability across all time domains. The lack of low frequency (greater than multi-decadal in periodicity) variability is consistent with previous published reconstructions based on the growth increment width chronologies (e.g. Reynolds et al., 2013). Whilst composite series derived from a spatial network may contain enhanced large scale climate signals, the variability contained in the reconstructions are limited to the portion of the frequency spectrum preserved in the individual chronologies. Growth increment width chronologies notoriously lack some low frequency variability because of the application of statistical detrending techniques for the removal of ontogenetic growth trends during chronology construction (Cook et al., 1995; Butler et al., 2010). This problem, termed the "segment length curse", is particularly prevalent in chronologies constructed from species with short lifespans. Relative to most tree-ring chronologies, the mean lifespan of bivalve specimens that make up the marine chronologies used in the generation of our composite series are short, limiting the low frequency variability that can realistically be reconstructed with these series to the multi-decadal scale. In order to reconstruct the complete spectrum of frequency domains alternative methodologies of producing the individual chronologies (prior to the construction of the composite series) are required. These include the use of annually resolved geochemical time series (Schöne et al., 2005), multiproxy techniques (Reynolds et al., 2013; Mette et al., 2016), or alternative detrending approaches (Nicault et al., 2010).

## 5. Conclusions

The results reported here demonstrate that composite series derived from annually resolved absolutely-dated sclerochronological networks can facilitate the robust reconstruction of large scale ocean variability and thereby have the potential to extend observational oceanographic (and climate) records over the past centuries. They also indicate that individual chronologies from climatically sensitive areas can also contain significant broad scale climate signals. Whilst the scarcity of long (multi-centennial to millennial) sclerochronological time series precludes the wider application of these methods at present, ongoing research will undoubtedly increase the availability of suitable shell-based chronologies and associated geochemical time series in the near future, leading to increasingly powerful high resolution reconstructions of past ocean variability.

## Acknowledgements

This work was supported financially by the NERC funded project Climate of the Last Millennium Project (CLAM; project No. NE/N001176/1) and the Marie Curie Frame work Partnership Annually Resolved Archives of Marine Climate Change (ARAMACC; Project No. FP7 604802). The authors would like to thank the three anonymous reviewer's for their constructive comments during the peer review process.

## Appendix A. Supplementary data

Supplementary data to this article can be found online at http://dx.doi.org/10.1016/j.palaeo.2016.08.006.

## References

Andreu, L., Planells, O., Gutierrez, E., Helle, G., Schleser, G.H., 2008. Climatic significance of tree-ring width and delta C-13 in a Spanish pine forest network. Tellus Ser. B Chem. Phys. Meteorol. 60, 771–781.

Black, B.A., 2009. Climate driven synchrony across tree, bivalve, and rockfish growth-increment chronologies of the northeast Pacific. Mar. Ecol. Prog. Ser. 378, 37–46.

Black, B.A., Boehlert, G.W., Yoklavich, M.M., 2008. A tree-ring approach to establishing climate-growth relationships for yelloweye rockfish in the northeast Pacific. Fish. Oceanogr. 5, 368–379.

Black, B.A., Copenheaver, C.A., Frank, D.C., Stuckey, M.J., Kormanyos, R.E., 2009. Multi-proxy reconstructions of northeastern Pacific sea surface temperature data from trees and Pacific geoduck. Palaeogeogr. Palaeoclimatol. Palaeoecol. 278, 40–47.

Black, B.A., Allman, R.J., Schroeder, I.D., Schirripa, M.J., 2011. Multidecadal otolith growth histories for red and gray snapper (Lutjanus spp.) in the northern Gulf of Mexico, USA. Fish. Oceanogr. 20, 347–356.

Black, B.A., Sydeman, W.J., Frank, D.C., Griffin, D., Stahle, D.W., Garcia-Reyes, M., Rykaczewski, R.R., Bograd, S.J., Peterson, W.T., 2014. Climate change. Six centuries of variability and extremes in a coupled marine-terrestrial ecosystem. Science 345, 1498–1502.

Briffa, K.R., Osborn, T.J., Schweingruber, F.H., Jones, P.D., Shiyatov, S.G., Vaganov, E.A., 2002a. Tree-ring width and density data around the Northern Hemisphere: part 1, local and regional climate signals. The Holocene 12, 737–757.

Briffa, K.R., Osborn, T.J., Schweingruber, F.H., Jones, P.D., Shiyatov, S.G., Vaganov, E.A., 2002b. Tree-ring width and density data around the Northern Hemisphere: part 2, spatio-temporal variability and associated climate patterns. The Holocene 12, 759–789.

Briffa, K.R., Osborn, T.J., Schweingruber, F.H., 2004. Large-scale temperature inferences from tree rings: a review. Glob. Planet. Chang. 40, 11–26.

Brocas, W.M., Reynolds, D.J., Butler, P.G., Richardson, C.A., Scourse, J.D., Ridgway, I.D., Ramsay, K., 2013. The dog cockle, *Glycymeris glycymeris* (L.), a new annually-resolved sclerochronological archive for the Irish Sea. Palaeogeogr. Palaeoclimatol. Palaeoecol. 373, 133–140.

Buntgen, U., Frank, D.C., Kaczka, R.J., Verstege, A., Zwijacz-Kozica, T., Esper, J., 2007. Growth responses to climate in a multi-species tree-ring network in the Western Carpathian Tatra Mountains, Poland and Slovakia. Tree Physiol. 27, 689–702.

Büntgen, U., Franke, J., Frank, D., Wilson, R., González-Rouco, F., Esper, J., 2010. Assessing the spatial signature of European climate reconstructions. Clim. Res. 41, 125–130.

Butler, P.G., Scourse, J.D., Richardson, C.A., Wanamaker Jr., A.D., Bryant, C.L., Bennell, J.D., 2009. Continuous marine radiocarbon reservoir calibration and the $^{13}C$ Suess effect in the Irish Sea: results from the first absolutely dated multi-centennial shell-based marine master chronology, Earth Planet. Sci. Lett. 279, 230–241.

Butler, P.G., Richardson, C.A., Scourse, J.D., Wanamaker, A.D., Shammon, T.M., Bennell, J.D., 2010. Marine climate in the Irish Sea: analysis of a 489-year marine master chronology derived from growth increments in the shell of the clam *Arctica islandica*. Quat. Sci. Rev. 29, 1614–1632.

Butler, P.G., Wanamaker, A.D., Scourse, J.D., Richardson, C.A., Reynolds, D.J., 2013. Variability of marine climate on the North Icelandic Shelf in a 1357-year proxy archive based on growth increments in the bivalve *Arctica islandica*. Palaeogeogr. Palaeoclimatol. Palaeoecol. 373, 141–151.

Cheng, W., Chiang, J.C.H., Zhang, D., 2013. Atlantic Meridional Overturning Circulation (AMOC) in CMIP5 models: RCP and historical simulations. J. Clim. 26, 7187–7197.

Cook, E.R., Briffa, K.R., Meko, D.M., Graybill, D.A., Funkhouser, G., 1995. The 'segment length curse' in long tree-ring chronology development for palaeoclimatic studies. The Holocene 5.

Cooper, R.J., Melvin, T.M., Tyers, I., Wilson, R.J.S., Briffa, K.R., 2013. A tree-ring reconstruction of East Anglian (UK) hydroclimate variability over the last millennium. Clim. Dyn. 40, 1019–1039.

Cunningham, L.K., Austin, W.E.N., Knudsen, K.L., Eiriksson, J., Scourse, J.D., Wanamaker Jr., A.D., Butler, P., Cage, A., Richter, T., Husum, K., Hald, M., Andersson, C., Zorita, E., Linderholm, H., Gunnarson, B.E., Sicre, M.A., Sejrup, H.P., Jiang, H., Wilson, R.J.S., 2013. Reconstructions of surface ocean conditions from the North East Atlantic and Nordic Seas during the last millennium. The Holocene 23, 921–935.

Ebisuzaki, W., 1997. A method to estimate the statistical significance of a correlation when the data are serially correlated. J. Clim. 10, 2147–2153.

Emanuel, K., 2005. Increasing destructiveness of tropical cyclones over the past 30 years. Nature 436, 686–688.

Folland, C.K., Palmer, T.N., Parker, D.E., 1986. Sahel rainfall and worldwide sea temperatures, 1901–85. Nature 320, 602–607.

Folland, C.K., Colman, A.W., Rowell, D.P., Davey, M.K., 2001. Predictability of northeast Brazil rainfall and real-time forecast skill, 1987–98. J. Clim. 14, 1937–1958.

Please cite this article as: Reynolds, D.J., et al., Reconstructing North Atlantic marine climate variability using an absolutely-dated sclerochronological network, Palaeogeogr. Palaeoclimatol. Palaeoecol. (2016), http://dx.doi.org/10.1016/j.palaeo.2016.08.006

Frank, D., Esper, J., 2005. Temperature reconstructions and comparisons with instrumental data from a tree-ring network for the European Alps. Int. J. Climatol. 25, 1437–1454.
Frankignoul, C., Czaja, A., L'Heveder, B., 1998. Air-sea feedback in the North Atlantic and surface boundary conditions for ocean models. J. Clim. 11, 2310–2324.
Goldenberg, S.B., Landsea, C.W., Mestas-Nunez, A.M., Gray, W.M., 2001. The recent increase in Atlantic hurricane activity: causes and implications. Science 293, 474–479.
Gray, S.T., 2004. A tree-ring based reconstruction of the Atlantic Multidecadal Oscillation since 1567 A.D. Geophys. Res. Lett. 31.
Haarsma, R.J., Hazeleger, W., Severijns, C., de Vries, H., Sterl, A., Bintanja, R., van Oldenborgh, G.J., van den Brink, H.W., 2013. More hurricanes to hit western Europe due to global warming. Geophys. Res. Lett. 40, 1783–1788.
Helama, S., Schone, B.R., Kirchhefer, A.J., Nielsen, J.K., Rodland, D.L., Janssen, R., 2007. Compound response of marine and terrestrial ecosystems to varying climate: pre-anthropogenic perspective from bivalve shell growth increments and tree-rings. Mar. Environ. Res. 63, 185–199.
Holliday, N.P., Cunningham, S.A., Johnson, C., Gary, S.F., Griffiths, C., Read, J.F., Sherwin, T., 2015. Multidecadal variability of potential temperature, salinity, and transport in the eastern subpolar North Atlantic. J. Geophys. Res. Oceans 120, 5945–5967.
Hurrell, J.W., 1995. Decadal trends in the North-Atlantic Oscillation - regional temperatures and precipitation. Science 269, 676–679.
Hurrell, J.W., Trenberth, K.E., 1999. Global sea surface temperature and analyses: multiple problems and their implications for climate analysis, modeling, and reanalysis. Bull. Am. Meteorol. Soc. 80, 2661–2678.
Inall, M., Gillibrand, P., Griffiths, C., MacDougal, N., Blackwell, K., 2009. On the oceanographic variability of the North-West European Shelf to the West of Scotland. J. Mar. Syst. 77, 210–226.
Jones, P.D., Jonsson, T., Wheeler, D., 1997. Extension to the North Atlantic Oscillation using early instrumental pressure observations from Gibraltar and south-west Iceland. Int. J. Climatol. 17, 1433–1450.
Knight, J.R., Folland, C.K., Scaife, A.A., 2006. Climate impacts of the Atlantic Multidecadal Oscillation. Geophys. Res. Lett. 33.
Lockwood, M., Harrison, R.G., Owens, M.J., Barnard, L., Woollings, T., Steinhilber, F., 2011. The solar influence on the probability of relatively cold UK winters in the future. Environ. Res. Lett. 6, 034004.
Lund, D.C., Lynch-Stieglitz, J., Curry, W.B., 2006. Gulf Stream density structure and transport during the past millennium. Nature 444, 601–604.
Mann, M.E., Zhang, Z., Rutherford, S., Bradley, R.S., Hughes, M.K., Shindell, D., Ammann, C., Faluvegi, G., Ni, F., 2009. Global signatures and dynamical origins of the little ice age and medieval climate anomaly. Science 326, 1256–1260.
Mann, M.E., Steinman, B.A., Miller, S.K., 2014. On forced temperature changes, internal variability, and the AMO. Geophys. Res. Lett. 41, 3211–3219.
Matta, M.E., Helser, T.E., Black, B.A., 2016. Otolith biochronologies reveal latitudinal differences in growth of Bering Sea yellowfin sole *Limanda aspera*. Polar Biol. http://dx.doi.org/10.1007/s00300-016-1917-y.
McGregor, H.V., Evans, M.N., Goosse, H., Leduc, G., Martrat, B., Addison, J.A., Mortyn, P.G., Oppo, D.W., Seidenkrantz, M.S., Sicre, M.A., Phipps, S.J., Selvaraj, K., Thirumalai, K., Filipsson, H.L., Ersek, V., 2015. Robust global ocean cooling trend for the pre-industrial Common Era. Nat. Geosci. 8 (671-+).
Mette, M.J., Wanamaker Jr., A.D., Carroll, M.L., Ambrose Jr., W.G., Retelle, M.J., 2016. Linking large-scale climate variability with *Arctica islandica* shell growth and geochemistry in northern Norway. Limnol. Oceanogr. 61, 748–764.
Moffa-Sánchez, P., Born, A., Hall, I.R., Thornalley, D.J.R., Barker, S., 2014. Solar forcing of North Atlantic surface temperature and salinity over the past millennium. Nat. Geosci. 7, 275–278.
Morice, C.P., Kennedy, J.J., Rayner, N.A., Jones, P.D., 2012a. Quantifying uncertainties in global and regional temperature change using an ensemble of observational estimates: the HadCRUT4 data set. J. Geophys. Res.-Atmos. 117.
Morice, C.P., Kennedy, J.J., Rayner, N.A., Jones, P.D., 2012b. Quantifying uncertainties in global and regional temperature change using an ensemble of observational estimates: the HadCRUT4 dataset. J. Geophys. Res. 117, D08101. http://dx.doi.org/10.1029/2011JD017187.
Nicault, A., Guiot, J., Edouard, J.L., Brewer, S., 2010. Preserving long-term fluctuations in standardisation of tree-ring series by the adaptative regional growth curve (ARGC). Dendrochronologia 28, 1–12.
North, G.R., Biondi, F., Bloomfield, P., Christy, J.R., Cuffey, K.M., Dickinson, R.E., Druffel, E.R.M., Nychka, D., Otto-Bliesner, B., Roberts, N., Turekian, K.K., Wallace, J.M., 2000. Surface Temperature Reconstructions for the Last 2,000 Years. The National Academies Press, New York.
Parker, D., Horton, B., 2005. Uncertainties in central England temperature 1878–2003 and some improvements to the maximum and minimum series. Int. J. Climatol. 25, 1173–1188.
Rahmstorf, S., Box, J.E., Feulner, G., Mann, M.E., Robinson, A., Rutherford, S., J., S.E., 2015. Exceptional twentieth-century slowdown in Atlantic Ocean overturning circulation. Nat. Clim. Chang.
Rayner, N.A., Parker, D.E., Horton, E.B., Folland, C.K., Alexander, L.V., Rowell, D.P., Kent, E.C., Kaplan, A., 2003. Global analyses of sea surface temperature, sea ice, and night marine air temperature since the late nineteenth century. J. Geophys. Res.-Atmos. 108.
Reynolds, D.J., Butler, P.G., Williams, S.M., Scourse, J.D., Richardson, C.A., Wanamaker, A.D., Austin, W.E.N., Cage, A.G., Sayer, M.D.J., 2013. A multiproxy reconstruction of Hebridean (NW Scotland) spring sea surface temperatures between AD 1805 and 2010. Palaeogeogr. Palaeoclimatol. Palaeoecol. 386, 275–285.
Ridgway, I.D., Richardson, C.A., Scourse, J.D., Butler, P.G., Reynolds, D.J., 2012. The population structure and biology of the ocean quahog, *Arctica islandica*, in Belfast Lough, Northern Ireland. J. Mar. Biol. Assoc. U. K. 92 (3), 539–546.
Robock, A., 2000. Volcanic eruptions and climate. Rev. Geophys. 38, 191–219.
Schmittner, A., Latif, M., Schneider, B., 2005. Model projections of the North Atlantic thermohaline circulation for the 21st century assessed by observations. Geophys. Res. Lett. 32.
Schöne, B.R., Fiebig, J., Pfeiffer, M., Gleβ, R., Hickson, J., Johnson, A.L.A., Dreyer, W., Oschmann, W., 2005. Climate records from a bivalved methuselah (*Arctica islandica*, Mollusca; Iceland). Palaeogeogr. Palaeoclimatol. Palaeoecol. 228, 130–148.
Smith, T.M., Reynolds, R.W., 2004. Improved extended reconstruction of SST (1854–1997). J. Clim. 17, 2466–2477.
Steinhilber, F., Beer, J., Fröhlich, C., 2009. Total solar irradiance during the Holocene. Geophys. Res. Lett. 36.
Sutton, R.T., Hodson, D.L.R., 2005. Atlantic Ocean forcing of North American and European summer climate. Science 309, 115–118.
Tandon, N.F., Kushner, P.J., 2015. Does external forcing interfere with the AMOC's influence on North Atlantic Sea surface temperature? J. Clim. 28.
Trenberth, K.E., Paolino, D.A., 1980. The Northern Hemisphere sea level pressure data set: Trends, errors, and discontinuities. Mon. Weather Rev. 108, 855–872.
Trenberth, K.E., Shea, D.J., 2006. Atlantic hurricanes and natural variability in 2005. Geophys. Res. Lett. 33.
Trouet, V., Van Oldenborgh, G.J., 2013. KNMI climate explorer: a web-based research tool for high-resolution paleoclimatology. Tree-Ring Res. 69, 3–13.
Trouet, V., Esper, J., Graham, N.E., Baker, A., Scourse, J.D., Frank, D.C., 2009. Persistent positive North Atlantic oscillation mode dominated the Medieval Climate Anomaly. Science 324, 78–80.
Trouet, V., Scourse, J.D., Raible, C.C., 2012. North Atlantic storminess and Atlantic Meridional Overturning Circulation during the last millennium: reconciling contradictory proxy records of NAO variability. Glob. Planet. Chang. 84-85, 48–55.
Wanamaker Jr., A.D., Butler, P.G., Scourse, J.D., Heinemeier, J., Eiriksson, J., Knudsen, K.L., Richardson, C.A., 2012. Surface changes in the North Atlantic Meridional Overturning Circulation during the last millennium. Nat. Commun. 3, 899.
Wigley, T.M.L., Briffa, K.R., Jones, P.D., 1984. On the average value of correlated time-series, with applications in dendroclimatology and hydrometeorology. J. Clim. Appl. Meteorol. 23, 201–213.
Wilson, R., Tudhope, A., Brohan, P., Briffa, K., Osborn, T., Tett, S., 2006. Two-hundred-fifty years of reconstructed and modeled tropical temperatures. J. Geophys. Res. Oceans 111, 13.
Wilson, R., Cook, E., D'Arrigo, R., Riedwyl, N., Evans, M.N., Tudhope, A., Allan, R., 2010. Reconstructing ENSO: the influence of method, proxy data, climate forcing and teleconnections. J. Quat. Sci. 25, 62–78.
Wilson, R., Anchukaitis, K., Briffa, K.R., Büntgen, U., Cook, E., D'Arrigo, R., Davi, N., Esper, J., Frank, D., Gunnarson, B., Hegerl, G., Helama, S., Klesse, S., Krusic, P.J., Linderholm, H.W., Myglan, V., Osborn, T.J., Rydval, M., Schneider, L., Schurer, A., Wiles, G., Zhang, P., Zorita, E., 2016. Last millennium northern hemisphere summer temperatures from tree rings: part I: the long term context. Quat. Sci. Rev. 154, 1–18.
Witbaard, R., Jansma, E., Sass Klaassen, U., 2003. Copepods link quahog growth to climate. J. Sea Res. 50, 77–83.

Please cite this article as: Reynolds, D.J., et al., Reconstructing North Atlantic marine climate variability using an absolutely-dated sclerochronological network, Palaeogeogr. Palaeoclimatol. Palaeoecol. (2016), http://dx.doi.org/10.1016/j.palaeo.2016.08.006